Russian Chemical Reviews **78** (9) 821 – 831 (2009) © 2009 Russian Academy of Sciences and Turpion Ltd

DOI 10.1070/RC2009v078n09ABEH004060

Nano-sized silicon carbide: synthesis, structure and properties

R A Andrievski

Contents

I.	Introduction	821
II.	Characteristic features of synthesis	822
III.	Structure and properties	826
IV.	Conclusion	830

Abstract. Characteristic features of the synthesis of particles, fibres (wires), tubes, films and bulk materials based on nanocrystalline and amorphous silicon carbide are considered. The role of size effects in the structure, composition and properties of these systems is analyzed. The potential application fields of nano-sized silicon carbide are outlined. The bibliography includes 83 references.

I. Introduction

Single-crystal and polycrystalline materials based on silicon carbide have long attracted attention of scientists for the wide spectrum of physicochemical and physicomechanical properties and, correspondingly, their wide application (*e.g.*, see the latest proceedings [1–3] of major international conferences carried out in 2006 – 2008). Certain data on nanocrystalline SiC published before 2005 were reported in reviews [4, 5] devoted to refractory compounds. However, both the number of publications on nano-SiC and the overall flow of information in the field of nanotechnology [6] show currently a trend to increase. According to information contained in the SCOPUS database, only in 2008, ~100 papers were devoted to nanocrystalline and amorphous objects based on SiC. In addition to the previously known characteristics of high stability and resistance to corrosion and radiation of silicon carbide and its promising high-temperature semiconductor behaviour, its attractive optical and biological properties were discovered. This altogether prompts an analysis of the latest trends in studies and engineering operations dealing with SiC-based nanomaterials. In the present review, attention is focused on the analysis of studies carried out in 2006 – 2009; moreover, as opposed to earlier publications,[4, 5] this review considers crystallographically amorphous compounds in addition to nanocrystalline objects, because silicon carbide exhibits a trend to amorphization. This is why, the name and the text of this review contain a term 'nano-sized' that combines the notions 'nanocrystalline' (nanostructural) and 'nanoamorphous' (*e.g.*, amorphous films with the thickness < 100 nm).

Silicon carbide crystallizes in numerous (more than 200) [7] different modifications (polylypes). Table 1 shows selected characteristics of the most abundant silicon carbide polytypes,[7–9] which makes easier further consideration and comparison of nanoobjects, and Fig. 1 demonstrates positions of carbon and silicon atoms in polytype structures. The composition of a silicon carbide polytype is determined first of all by the conditions of synthesis (temperature, pressure, environment) and the presence of impurities. The cubic polytype 3*C*-SiC (β-SiC) is assumed to be more stable than hexagonal polytypes (up to ~2100 °C).[8] The 2*H* polytype is the most unstable. In addition to the cubic polytype and three hexagonal versions, silicon carbide is

Table 1. Basic physicochemical characteristics of the most abundant silicon carbide polytypes.[7–9]

Polytype characterization	3*C*-SiC (β-SiC)	2*H*-SiC (α-SiC)	4*H*-SiC (α-SiC)	6*H*-SiC (α-SiC)
Structural group	$F\bar{4}3m$	$P6_3mc$	$P6_3mc$	$P6_3mc$
Hexagonality (%)	0	100	50	33
Layer alternation (see Fig. 1)	ABC	AB	ABCB	ABCACB
Lattice spacing /nm				
a	0.43589 – 0.43596	0.30753 – 0.3081	0.3070 0.3081	0.3073 – 0.3081
c	–	0.5031 – 0.5048	1.0053 – 1.008	1.51092 – 1.512
Tabulated values /nm				
a	0.4359	0.3079	0.3073	0.3080
c	–	0.5053	1.053	1.5117
Density /g cm^{-3}	3.215	3.219	3.215	3.212
Band gap /eV	2.39	3.33	3.26	3.02
Electron mobility at 300 K /cm^2 V^{-1} s^{-1}	⩽1000	–	⩽850	⩽450
Hole mobility at 300 K /cm^2 V^{-1} s^{-1}	⩽40	–	⩽120	⩽100

R A Andrievski Institute of Problems of Chemical Physics, Russian Academy of Sciences, prosp. Akad. Semenova 1, 142432 Chernogolovka, Moscow Region, Russian Federation. Fax (7-496) 522 35 07, tel. (7-496) 522 77 93, e-mail: ara@icp.ac.ru

Received 8 April 2009
Uspekhi Khimii **78** (9) 889 – 900 (2009); translated by T Ya Safonova

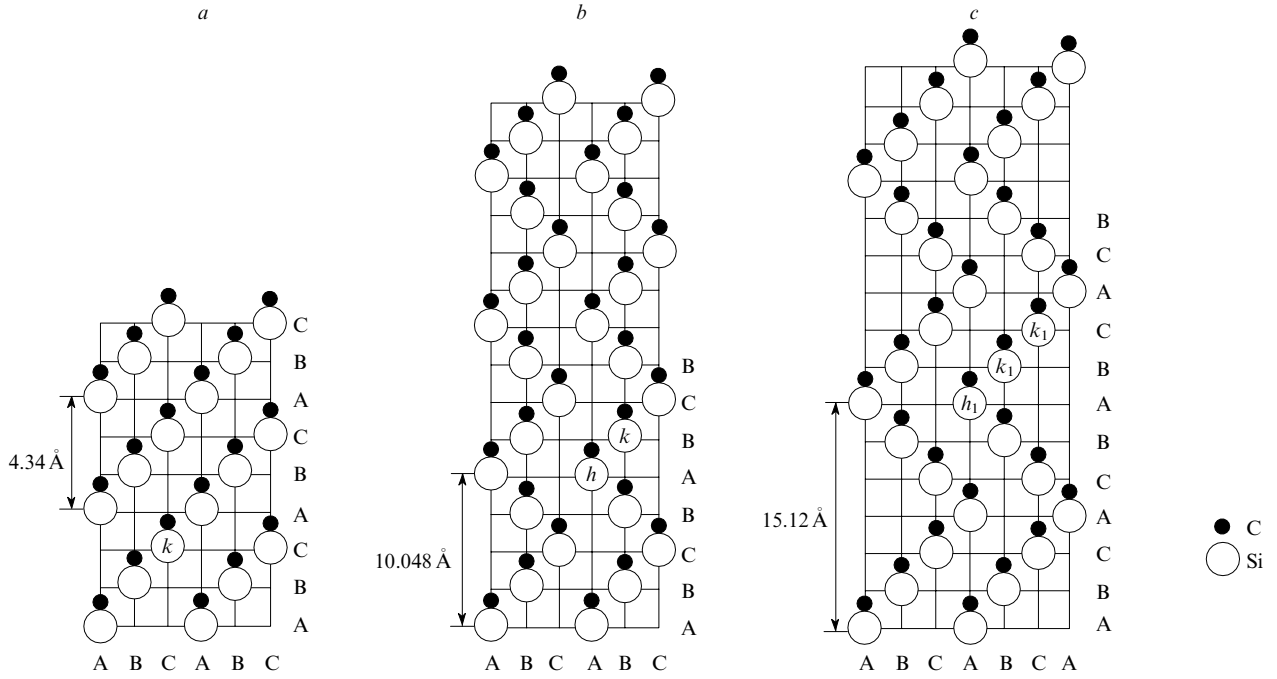


Figure 1. Positions of carbon and silicon atoms $(11\bar{2}0)$.[7] (*a*) 3*C*-SiC, (*b*) 4*H*-SiC, (*c*) 6*H*-SiC.

also characterized by the fifteen-layer rhombohedral polytype 15*R* (structural group *R*3*m*, the band gap 2.99 eV). Different electrophysical characteristics of silicon carbide polytypes make them promising precursors for the design of heterostructures, which makes elucidation of the effect of size-dependent factors on the properties of SiC especially challenging.

II. Characteristic features of synthesis

1. Nanopowders, nanoparticles in matrices, nanoporous structures, nanowires and nanotubes

Silicon carbide nanopowders are manufactured by different companies. For instance, PlasmaChem GmbH (Germany) supplies SiC nanopowder with the average particle size of 20 ± 7 nm and $> 95\%$ purity (free silicon content $< 0.75\%$, oxygen content $< 1.25\%$, chlorine content $< 0.25\%$).

In recent publications on the synthesis of SiC nanopowders, the peculiarities of tetramethylsilane decomposition in microwave low-pressure plasma to afford crystallographically amorphous nanoparticles with sizes 4–6 nm were investigated,[10] the effect of the pre-reaction mechanical activation treatment on the kinetics of silicon and carbon combustion in air in the synthesis of the β-SiC powder was revealed,[11] the grain size of powders prepared by a furnace and microwave synthesis was compared.[12]

These studies continued and, to a certain extent, refined earlier investigations of the carbothermal, plasmochemical and laser syntheses reflected in reviews.[4,5] At present, attention of scientists is focused on the synthesis of nano-sized SiC particles in matrices and also of silicon carbide nanowires and nanotubes. The following major technological methods were used: electrochemical and chemical etching, carbidization of silicon and its oxide, implantation of carbon ions into silicon, co-implantation of carbon and silicon ions into SiO_2-type matrices. The methods of synthesis of nano-sized silicon (a material for nanoelectronics) were considered in a monograph[13] and the synthesis of nano-sized SiC was the subject of a review,[14] which summarizes the results of studies carried out up to 2005 and also contains a detailed discussion of specific features of technological processes.

For nanoporous Si and SiC, intensification of photoluminescence (PL) was observed.[13] Figure 2 shows low-temperature PL spectra for a silicon carbide support, a porous SiC layer and SiC nanoparticles measuring < 10 nm.[15] The increase in PL for the last two objects is clearly observed, particularly, for isolated nanoparticles. Whereas the original 6*H*-SiC sample was characterized by

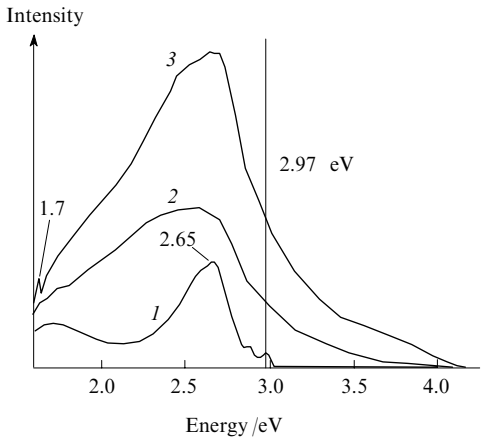


Figure 2. Photoluminescence spectra of a standard 6*H*-SiC substrate (*1*), nanoporous SiC layer synthesized by substrate anodization (*2*) and SiC nanoparticles prepared by intense grinding of the nanoporous layer (*3*).[15]
Photoluminescence was measured ($T = 9$ K) at the 5.08 eV line excitation with an argon laser. The figure also shows the band gap (2.97 eV) for the 6*H*-SiC prototype and the energy of PL peaks.

relatively weak emission in the energy range of 1.7–2.6 eV, the porous sample after etching and isolated nanoparticles exhibited intense luminescence in the wider energy range from 1.6 to 3.5 eV, which was associated with the quantum-size effect. Presumably, considerable contribution to the PL gain was made by the defective surface structure of nanopores formed in the etching.[14]

Electrochemical anodic etching was carried out at a current density of 210 mA cm^{-2} in an HF–EtOH (1 : 1) solution for 25 min; the porous layer ($\sim$100 μm thick) was separated from the support by short-term increase in the current density to 1 A cm^{-2} (Ref. 15). Moreover, it was reported[16] that common 3*C*-SiC powders can be disintegrated (from particles of several microns to nanoparticles measuring several nanometres) by chemical etching in the HNO_3–HF (1 : 3) mixture at 100 °C for 1 h, followed by centrifugation, washing and drying. Figure 3 shows an electron microscopic image of SiC nanocrystals, a histogram of their size distribution and also an image of a single nanoparticle.[16] It is seen that the obtained nanoparticles are round-shaped and sufficiently size-uniform (average size of 3.75 nm).

The technology of fabrication of porous silicon carbide samples usually combined the SiC synthesis with the formation of a porous skeleton, which made it possible to considerably decrease the temperature and build structures with fine pores. Thus heating of a mixture of silicon powder with fullerenes or carbon black in sodium vapour (which favours mass transfer) at $\sim$700 °C afforded β-SiC with $\sim$70% porosity that contained pores 2–10 nm in diameter and nano-sized crystals.[17] Pyrolysis of polycarbosilanes mixed with nano-sized SiC powder afforded mesoporous samples.[18] It was proposed to obtain porous materials based on SiC nanowires ($\sim$100 nm in diameter, several tens of micrometres long) by the carbothermal reduction of SiO_2.[19]

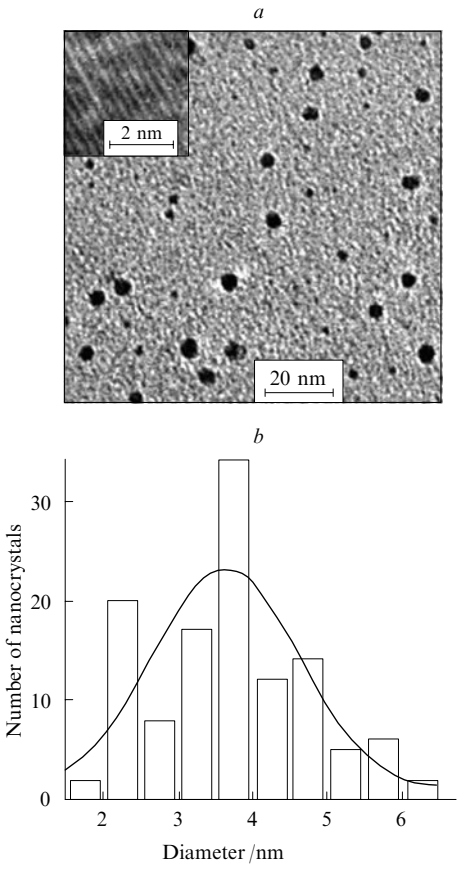


Figure 3. Bright-field electron microscopic image of SiC nanocrystals in ethanol medium (*a*) and their size distribution (*b*).[16]
Inset shows a high-resolution image of a nanoparticle, namely, the {111} planes of cubic SiC.

Studying carbidization of porous silicon synthesized by electrochemical etching demonstrated[20] the formation of 3*C*-SiC nanocrystals measuring 5–7 nm at 1200–1300 °C. It was assumed that peculiarities of the mechanism of this process favoured the formation of a heterostructure that simultaneously included silicon nanocrystals and nano-sized particles of amorphous SiC.

Several publications (*e.g.*, see Refs 14, 21–23) dealt with specific features of the implantation (ion-beam) synthesis of SiC nanoparticles. In a pioneering study,[21] it was found that implantation of carbon ions (dose 10^{17} cm^{-2}, energy 50 keV) into a silicon substrate followed by thermal annealing and electrochemical etching was accompanied by the appearance of β-SiC nanocrystals measuring $\sim$2–5 nm and gave rise to a new peak in the PL spectrum in the vicinity of 445 nm (2.79 eV, see Fig. 2) with the intensity 2.7-fold higher as compared with the PL peak of the substrate subjected to similar treatment but without carbon implantation. The effects of the radiation dose, temperature and the annealing time on the structure and optical properties of synthesized SiC nanocrystals were studied, which included both the individual implantation of carbon or silicon ions and the stepwise double implantation of these ions using SiO_2 films as the substrates.[14,23] In the latter case, the data from EPR, XPS, PL spectroscopy, high-resolution transmission electron microscopy (HRTEM), *etc.*, revealed the presence of several crystalline and amorphous nanoinclusions of silicon, silicon carbide and carbon measuring $\sim$5 nm formed as a result of implantation and additional annealing. Their formation mechanism is complicated and still much unclear. The advantages of implantation synthesis include its compatibility with the conventional silicon planar technology and also the predicted high chemical and mechanical stability of SiC nanoparticles incorporated into a wide-band SiO_2 matrix.

Silicon ion implantation (doses in the range from 10^{16} to 2×10^{17} ions cm^{-2}, energy of 40 keV) into carbon nanotubes was studied.[24] The structure and composition of implanted tubes were explored by the HRTEM, XPS, energy dispersive X-ray spectroscopy (EDS) and other methods that revealed the formation of crystallographically amorphous silicon carbide the crystallization of which required addition annealing.

Some studies (see, *e.g.*, Refs 25–28) are devoted to fabrication of silicon carbide nanowires and nanotubes by direct synthesis, *i.e.*, as a result of the reaction of silicon (or its monoxide) vapour with carbon. The synthesis of SiC proceeds by the following reactions:[25,27,28]

$$2\,C\,(s) + O_2 = 2\,CO, \quad (1)$$

$$2\,Si\,(g) + O_2 = 2\,SiO\,(g), \quad (2)$$

$$SiO\,(g) + 2\,C\,(s) = SiC\,(s) + CO, \quad (3)$$

$$SiO\,(g) + CO = SiC\,(s) + O_2, \quad (4)$$

$$3\,SiO\,(g) + 3\,C\,(s) = 2\,SiC\,(s) + SiO\,(s) + CO_2, \quad (5)$$

$$SiO\,(g) + 3\,CO = SiC\,(s) + 2\,CO_2, \quad (6)$$

Table 2. Characteristics of SiC nanowires.

Synthesis time /h	Diameter /nm	Length /μm	Cross-section shape	Phase composition	Photoluminescence presence	Ref.
4 – 9	~200	10 – 20	hexagonal	β-SiC	not observed	25
2	50 – 200	several tens	"	traces α-SiC, C and O; SiO_2 shell	peaks at 289 and 391 nm	26
1	60 – 100	several units	circular	β-SiC; SiO_2 shell	not observed	27

$$CO_2 + C\,(s) = 2\,CO, \quad (7)$$

$$3\,SiO\,(g) + CO = SiC\,(s) + 2\,SiO_2\,(s), \quad (8)$$

$$4\,CO + 6\,Si\,(s) = 4\,SiC\,(s) + 2\,SiO_2\,(s). \quad (9)$$

In some of these reactions, CO, SiO and SiO_2 are regenerated. The realization of one or another reaction scheme depends on the temperature and the degree of supersaturation; however, virtually no detailed studies of these reactions were aimed at elucidation of their stages and mechanisms.

It was noted that the synthesis of SiC nanowires by evaporation at 1600 °C in the argon atmosphere may involve the use of different starting components, namely, silicon in a graphite crucible and a graphite substrate [reactions (1) – (4)];[25] a mixture of silicon and ball-milled activated carbon and a mixture of silicon monoxide powder and arc-discharge plasma pretreated carbon black [reactions (5) – (8)].[27] The results of these studies aimed at the large-scale synthesis can be compared using the data from the Table 2. All technological processes were carried out in the absence of catalysts, *i.e.*, the most probable growth mechanism may be represented by the vapour → solid scheme (in the absence of liquid phase); the crystal growth proceeded in the ⟨111⟩ direction. Figure 4 shows the appearance of SiC nanowires with hexagonal and core-shell structures. The presence of a silica shell can be distinguished (see Fig. 4 *b*,*c*); according to the data of X-ray diffraction analysis, silica was in the crystallographically amorphous state.

Evidently, the nature of starting components considerably affects the synthesis processes; however, it is difficult to choose the synthesis method due to scarce information on the composition and properties of the final product.

The use of a nickel catalyst allowed reduction of the temperature of formation of nanowires with the 3*C*-SiC structure to 1050 – 1100 °C in the reaction of CO with the SiO_2/Si interface [reaction (9)].[28]

β-SiC nanotubes can also be synthesized by different methods, for example, by the reaction of SiO vapour with carbon nanotubes at 1200 °C for 100 h (Ref. 29) or by the reduction of methyltrichlorosilane with hydrogen in the presence of a catalyst (ferrocene) at 1000 °C for 1 h.[30] The outer diameter of nanotubes was 20 – 80 nm, the inner diameter varied from 15 to 35 nm.[30] A detailed thermodynamic analysis of the gas-phase reactions in chemical vapour deposition of SiC with methyltrichlorosilane precursor was carried out.[31] It was shown that in the synthesis of β-SiC, the optimal temperature of the reduction of Me_3SiCl with hydrogen was ~1200 °C.

2. Films and compacts

The synthesis of nano-sized (crystalline and amorphous) SiC involved the use of physical and chemical vapour deposition (PVD and CVD versions): reactive magnetron synthesis with carbon and silicon targets, non-reactive magnetron synthesis with a silicon carbide target, hybrid laser-magnetron synthesis, pulsed laser synthesis, electron-beam evaporation, plasma-enhanced CVD, *etc.* (see, *e.g.*, Refs 32 – 41). In addition, sublimation methods and molecular-beam epitaxy were used.[7] Nitrogen-doped SiC films can be obtained if ammonia was added into the gaseous precursor ($SiH_4 + C_2H_2$ mixture);[39] in the synthesis of composite films of the β-SiC – diamond type, the composition of the gaseous precursor ($H_2 + CH_4 + SiMe_4$ mixture) was varied.[41]

Table 3 contains certain examples of magnetron synthesis and chemical vapour deposition. Considering these data, it should be noted that in the overwhelming majority of cases, the freshly deposited SiC films were crystallographically amorphous. Their transition into the crystalline state required higher temperatures of the substrates or additional annealing. The structural state of films was usually determined using the XRD (diffractometers with grazing incidence beam in the low-angle range were used to enhance the sensitivity) and TEM methods, by analyzing the Fourier transform IR (FTIR) and Raman spectra and also XPS. The film composition was studied by XPS, EDS, Rutherford backscattering spectroscopy, Auger electron spectroscopy and electron energy loss spectroscopy.

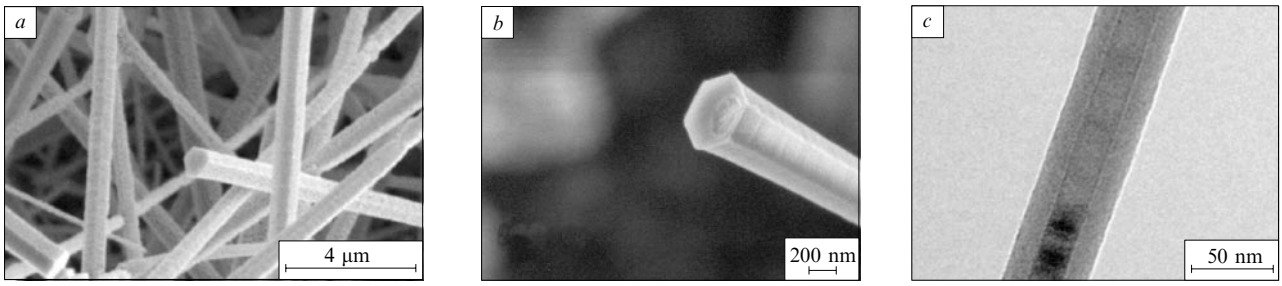


Figure 4. SiC Nanowires according to the results of high resolution transmission electron microscopy (HRTEM). (*a*), (*b*) and (*c*) correspond to the results obtained in Refs 25, 26, 27, respectively.

Table 3. Characteristics of different methods of SiC synthesis.

Synthetic method	Annealing temperature /°C	Phase composition	Grain size /nm	Study method	Ref.
Reactive magnetron synthesis using C and Si targets (Si substrate)	1100	β-SiC	7.3 ± 0.4 3 – 10	X-ray diffraction analysis HRTEM	32
Reactive magnetron synthesis (ion energy ~90 eV; Si, Al_2O_3, Mo, SiO_2 substrates, deposition temperature 700 – 1050 °C)	950 1140	80% β-SiC 85% (α + β)-SiC	8 – 10 17	X-ray diffraction analysis photoelectron spectroscopy	33
Reactive magnetron synthesis in the H_2 + Ar mixture at 200 – 600 °C; Si substrate	–	3*C*-SiC + 6*H*-SiC	4 – 5	HRTEM	35
Plasma-activated deposition from $CH_4 + SiH_4$ + Ar mixture on Si and SiO_2 substrates at 350 °C	1300	2*H*-SiC + 4*H*-SiC	15 5	HRTEM X-ray diffraction analysis	36
Deposition from $SiH_4 + CH_4 + H_2$ mixture on a molybdenum wire at 100 – 430 °C	–	3*C*-SiC	6 – 12	X-ray diffraction analysis	37

Figure 5 shows examples of the temperature evolution of the Raman, XRD and IR spectra for SiC films synthesized by reactive magnetron sputtering in the argon [32] and hydrogen – argon plasma [35] and also by CVD onto a molybdenum wire from a mixture of silane, methane and hydrogen.[37] The characteristic features of these spectra were discussed in detail [34] as applied to films, nanowires, nanoneedles and other SiC nanoobjects synthesized on silicon

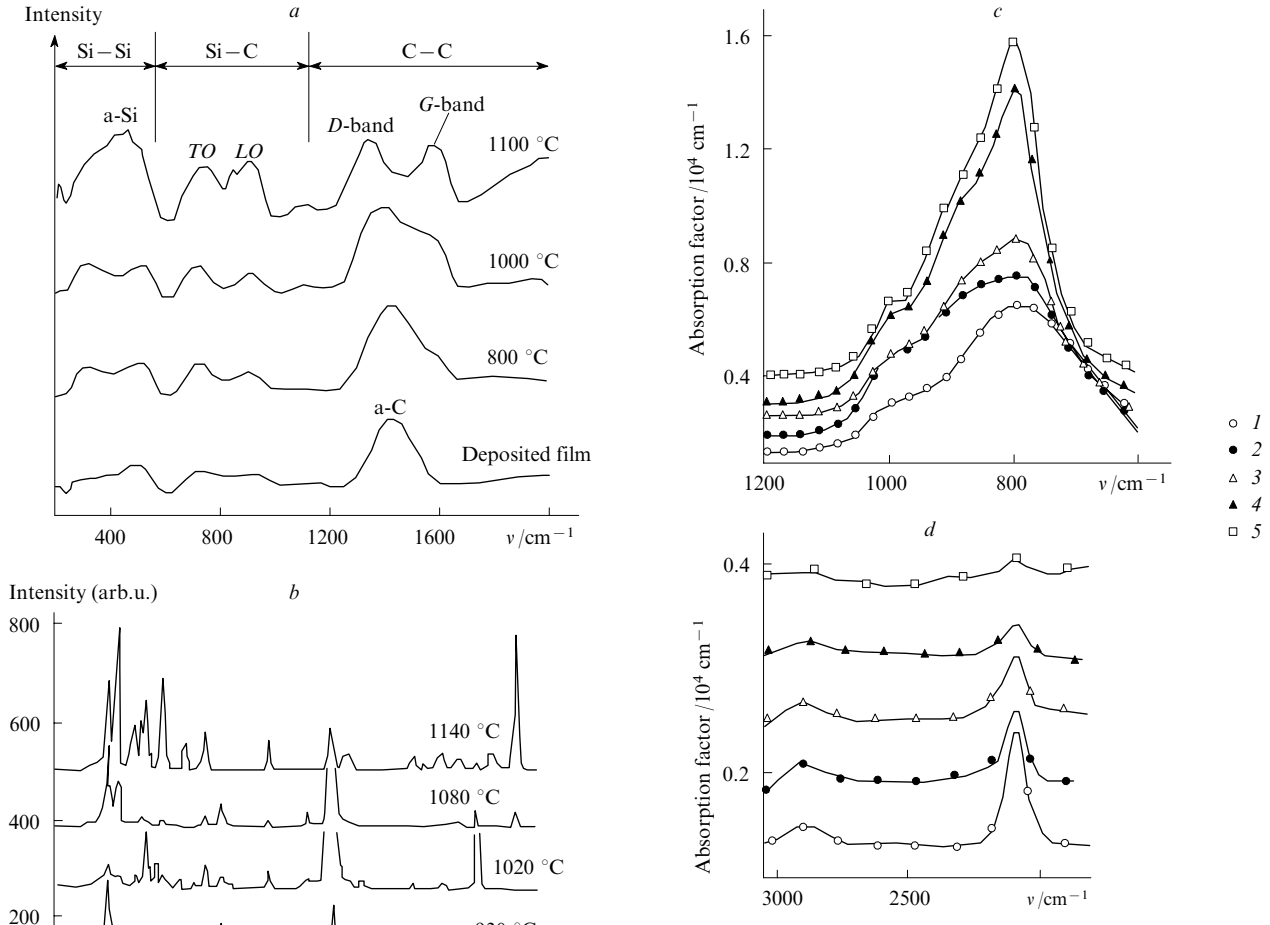


Figure 5. The effect of annealing temperature on the Raman (*a*),[32] XRD (*b*)[33] and different-range IR (*c*, *d*) spectra.[35]
(*a*) a-Si and a-C are amorphous silicon and carbon; *TO* and *LO* are the transverse and longitudinal modes; *D*-band and *G*-band are *D* and *G* vibration modes in the carbon sublattice. (*c*, *d*) *T*/°C: 200 (*1*), 300 (*2*), 400 (*3*), 500 (*4*), 600 (*5*).

substrates by pulsed laser irradiation. Particularly, the presence of small reflexes in the vicinity of the pronounced (111) peak in β-SiC XRD patterns was mentioned, which was associated with stacking defects. At the same time, the Raman spectra demonstrated peculiarities as compared with those observed earlier,[32] for example, the presence of peaks at 972 and 800 cm^{-1}.

Various temperature conditions of crystallization of a particular SiC polytype depend on experimental conditions and many kinetic parameters. Different temperature dependences of the grain size were also typical, for instance, a non-monotonic dependence with a maximum at 280 °C observed in experiments on vapour deposition from the $SiH_4 + CH_4 + H_2$ mixture,[37] monotonic size variations with the increase in the temperature of co-deposition of carbon and silicon ions[33] and an athermic dependence in the interval of 200 – 600 °C for reactive magnetron sputtering.[35] These data altogether necessitate further studies with the aim of refining various mechanisms of SiC film formation.

A method of solid-state epitaxy of SiC on silicon was developed, which consists of treating single-crystal silicon with carbon monoxide ($T = 1100 - 1400$ °C, $P_{CO} = 10 - 300$ Pa, $t = 5 - 60$ min).[42] It was assumed that vacancies and pores near the interface between SiC and Si as a result of this reaction due to the formation and removal of gaseous SiO provided relaxation of elastic stresses caused by the lattice misfit between silicon and silicon carbide. This resulted in the epitaxial growth of 20 – 100 nm thick SiC films on silicon. A thermodynamic nucleation theory developed for this case and a model of stress relaxation by vacancies and pores in the substrate was put forward. Experiments have shown that the films were formed based on 4*H* or 3*C* polytypes and also on their mixtures. Figure 6 demonstrates the PL spectra of 4*H* and 3*C* polytypes; peaks correspond to wavelengths of ~380 and ~540 nm (6*H* polytype has a peak at a wavelength of ~430 nm). The PL spectrum for cubic polytype was close to the blue emission.

Liquid-phase epitaxy of 2*H*-SiC films on the 4*H*-SiC substrate (0001) in a Li – Si melt at 850 °C ($t = 48$ h) was documented.[43]

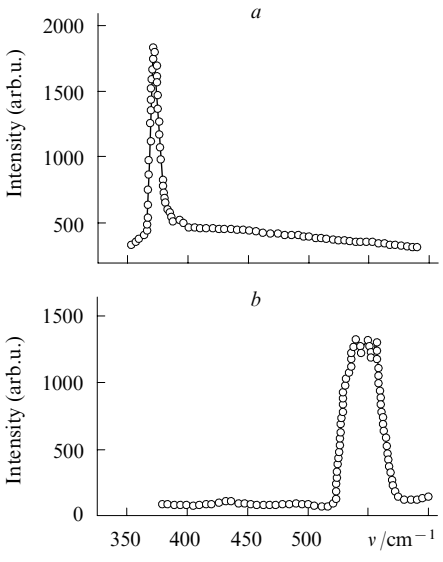


Figure 6. Photoluminescence spectra of 4*H*-SiC (*a*) and 3*C*-SiC (*b*) polytypes at 77 K.[42]

In contrast to the synthesis of nano-sized SiC films, attempts to prepare bulk nanomaterials were less successful.[4, 5, 44] Preparation of bulk nanostructured materials was hampered by the intensive recrystallization of nanopowders at consolidation temperatures. Even the recourse to high-pressure and high-temperature technique (sintering at pressures > 1 GPa) to fabricate SiC samples with the crystal size less than ~20 nm met with difficulties. The examples of preparation of compact samples by sintering of SiC nanopowders activated by mechanosynthesis, as well as of highly porous materials of highly dispersed mixtures of carbon and silicon are known.[4]

III. Structure and properties

1. Structural peculiarities and composition

According to the literature data, different SiC polytypes are characterized by different stoichiometric ratios and concentrations of carbon vacancies (Table 4).[45] Structural studies of nano-SiC polytypes were insufficiently detailed to draw conclusions on the effect of size on the deviations from stoichiometry and vacancy characteristics. For nano-SiC of the cubic polytype, the following values of lattice spacing (a/nm) are known: 0.436 (grains of 4 – 7 nm);[17] 0.4353 (nanowire 200 nm in diameter);[25] 0.4370 (nanowire 60 – 100 nm in diameter);[27] 0.4361 (nanowire 60 – 70 nm in diameter);[28] 0.438 (crystal size 2 – 5 nm).[35] For the 6*H* polytype, $a = 0.309$, $c = 1.525$ nm.[35] The majority of these values are comparable with the data in Table 1; however, it is difficult to judge on how the size factor or impurities affect the lattice spacing, although it was noted[35] that the lattice spacing in nanoinclusions of α- and β-polytypes increased as compared with lattice constants of their bulk analogues.

Table 4. Ratio Si : C and averaged concentration of carbon vacancies (N_C) in different SiC polytypes.[45]

Polytype	Si : C	$N_C/10^{20}$ cm^{-3}
3*C*	1.046	33.6
6*H*	1.022	16.3
15*R*	1.012	15.1
4*H*	1.001	7.3

Evolution of carbon, argon and hydrogen in the annealing of amorphous and nanocrystalline SiC films was studied by several authors (see, *e.g.*, Refs 33, 34, 36, 46, 47). The temperature variations in the Si – Si, C – C and Si – C interatomic interactions were followed and the changes in the film composition and structure were revealed using XRD, HRTEM, IR spectroscopy and other methods. The EDS method for samples obtained by pulsed laser deposition technique revealed changes in the contents of carbon and silicon.[34]

The excessive amount of silicon was attributed to the effect of the silicon substrate; the presence of oxygen admixtures was also mentioned.

T/°C	500	1000	1200
C content (at.%)	24.18	17.95	15.20
Si content (at.%)	75.65	81.12	83.51

Figure 7 shows HRTEM images of cross-sections of SiC films deposited by reactive magnetron sputtering in hydrogen-argon plasma at different silicon substrate tempera-

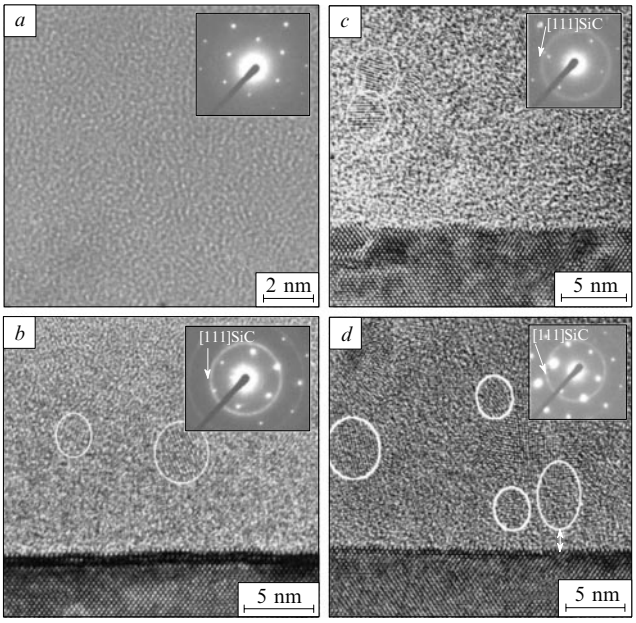


Figure 7. The effect of silicon substrate temperature on the crystallization of an amorphous SiC film (HRTEM data).[35]
T/°C: 200 (*a*), 300 (*b*), 400 (*c*), 600 (*d*). Insets show electron micropatterns; nanograins in reflection positions are encircled.

tures.[35] As can be seen (considering also diffraction micropatterns given in insets), the crystallization of SiC nanoinclusions (6*H* or 3*C* polytypes) in the amorphous matrix intensifies as the temperature increases; the same correlation was observed in the evolution of IR spectra (see Fig. 5 *c*). Analysis of the acquired information has shown that the structure contains stacking faults and twins. The TEM and HRTEM studies of the defectiveness of β-SiC layers grown by the CVD technology on a silicon (001) substrate with a propane-silane precursor ($C_3H_8 + SiH_4$) also revealed the presence of stacking faults and twins.[48] The origin of these planar defects was associated with both peculiarities of the crystal growth on the SiC/Si interface and the low energy of stacking defects in silicon carbide. The role of size effects in energy variations of stacking defects in nano-sized SiC was analyzed.[49]

The presence of pores, the formation of different polytypes, their subsequent coalescence and the manifestation of stacking defects were observed in SiC films synthesized by the solid phase epitaxy method.[50]

The morphology of growing SiC nuclei was successfully followed by atomic force microscopy (AFM). Figure 8 exemplifies their nucleation observed after carbon was deposited on a silicon substrate by the electron-beam evaporation method.[51] These nuclei represented cones with the base of the average radius of ~70 nm and the average height of ~4 nm; their surface density was ~10^9 cm^{-2}. Using a molecular dynamics method (computations), a physical model describing the formation and growth of such nuclei during molecular-beam epitaxy was developed.[52] Theoretical estimates of the time of transition from two- to three-dimensional growth agreed with experimental results.

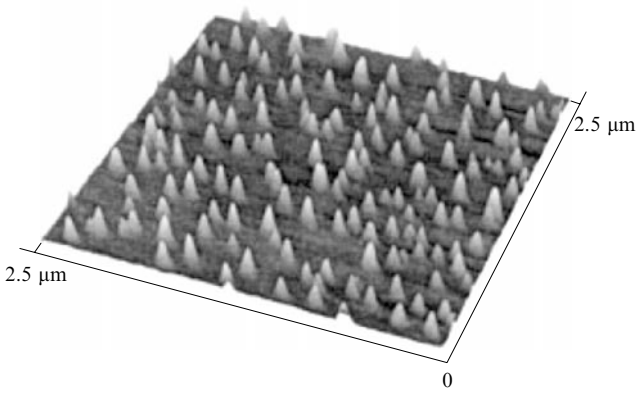


Figure 8. AFM Images of SiC nuclei formed by carbon vapour deposition.[51]
Flow 5×10^{13} cm^{-2} s^{-1}; T = 925 °C; t = 10 s

2. Properties

The effect of temperature of magnetron sputtering and subsequent annealing on the properties of 3.2–4.4 μm thick SiC films is illustrated by the data shown in Table 5 and Fig. 9.[47] For comparison, Table 5 lists the properties of sintered and single-crystalline SiC samples. As was mentioned above, the deposited SiC films were crystallographicaly amorphous and characterized by the high argon content and considerable intrinsic stresses (arising due to the difference in properties of the silicon substrate and the growing SiC layers). It is evident that as the temperatures of deposition and subsequent annealing increased, the argon content decreased, the intrinsic stresses in films were relieved and their elastic moduli and hardnesses increased. When heated, the amorphous films gradually crystallized and, according to the HRTEM data (see Fig. 7), the progressive formation of β-SiC crystals measuring 1–6 nm was

Table 5. Phase composition, elastic modulus and hardness of SiC films synthesized under different temperature conditions.[47]

T_{sub}/°C	T_{ann}/°C	Phase composition	E/GPa	H/GPa
25	–	amorphous phase	280 ± 5	22.2 ± 0.2
	800	the same	312 ± 6	28.9 ± 0.7
	1000	"	331 ± 3	34.1 ± 2.1
	1200	" (see [a])	365 ± 6	36.3 ± 2.0
400	–	"	283 ± 5	27.0 ± 0.4
600	–	"	297 ± 3	30.5 ± 0.4
750	–	amorphous phase + β-SiC	378 ± 3	40.0 ± 1.0
	800	amorphous phase + β-SiC (L ~ 6 nm)	369 ± 3	39.5 ± 0.5
	1000	amorphous phase + β-SiC	374 ± 2	37.8 ± 0.5
750 [b]	–	amorphous phase + β-SiC (L ~ 3 nm)	385 ± 2	40.5 ± 0.8
	800	amorphous phase + β-SiC (L ~ 6 nm)	367 ± 2	40.9 ± 0.8
		polycrystalline sintered SiC	312 ± 7.5	21.6 ± 1.0
		single crystal α-SiC (0001)	499 ± 2.0	36.0 ± 2.0
		single crystal β-SiC (111)	440 ± 16	32.0 ± 2.0

Notes. The following designation are taken: T_{sub} is the substrate temperature, T_{ann} is the temperature of additional vacuum annealing for 1 h, E is the elastic modulus, H is the hardness, L is the crystal size.
[a] Traces of nanocrystallization. [b] Deposition with negative bias voltage applied to the substrate.

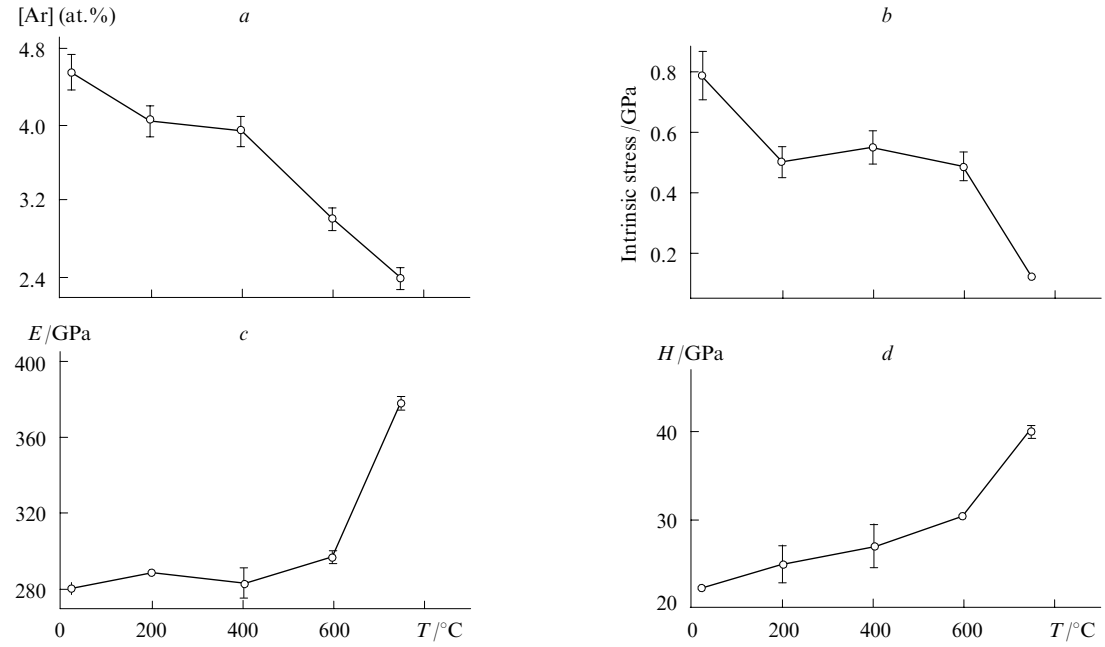


Figure 9. The effect of substrate temperature on the argon content (*a*), intrinsic stress (*b*), elasticity modulus (*c*) and hardness (*d*) of SiC films.[47]

observed starting from ~300 °C (in Ref. 47, the XRD experiments revealed the formation of nanocrystals at temperatures above ~700 °C). The film properties strongly depended on the negative bias voltage applied to the substrate. Thus, the increase in the elastic modulus and hardness was the result of action of many factors (phase composition variations with the increase in the number of nanocrystals, chemical composition refining, changes in the strained state, *etc*.); hence, it is difficult to single out their individual roles.

A comparison of coarsely crystalline and single-crystalline films has shown that hardnesses and elastic moduli for SiC samples with the amorphous nanocrystalline structure are lower than those for common sintered samples and, especially, single crystals. This can be explained by considerable content of the amorphous phase in films that escaped complete nanocrystallization during the synthesis.[47]

The role of size effects in hardness and elastic modulus of nano-SiC is also illustrated by the data from Table 6. It is evident that, as for other nanomaterials,[4, 5, 57] a decrease in the grain size results in an increase in H due to the progressive effect of intergrain boundaries, *i.e*., barriers to propagation of dislocations and cracks. A decrease in E observed for different materials with the crystal size at a level $< 30-50$ nm was associated with the lower fraction of intergrain boundaries the elasticity characteristics of which are inferior to those for the regular crystalline state.[57] In the most general form, the properties of nano-SiC should depend not only on the grain size, but also on the crystallinity of the structure, *i.e*., the fraction of the amorphous component and also on the particular properties and composition of these components. It is common practice to analyze the properties of amorphous nano-SiC-based composites by comparing them with the ratios of sp^3 and sp^2 carbon atoms retrieved from the results of the Raman and XPS studies (recall that the sp^3 configuration corresponds to diamond and sp^2 configuration corresponds to graphite; for example, see Ref. 55).

Table 6. The effect of crystal size on the hardness and elastic modulus.

L /nm	H /GPa	E /GPa	Notes	Ref.
~10	~50	~515	films synthesized in hydrogen–silane microwave plasma on molybdenum substrates at ~1200 °C; crystallinity ratio ~85%; residual stresses is 0.25 GPa	53
~13	55.0 ± 10.5	425 ± 84	films synthesized by electron-beam evaporation on stainless steel substrates at 900 °C	54
~20	~37	–	films prepared in supersonic plasma	55
~70	24–25	–	compacts prepared by hot isostatic pressing of nano-powders	56

On this evidence it is clear that the discerning of contributions of different factors in the $H = f(L)$ and $E = f(L)$ dependences for SiC-based nanomaterials requires additional studies. Nonetheless, it is evident that with a decrease in the grain size, the hardness of SiC and other refractory compounds substantially increased.[4, 5] Preliminary results pointed to a considerable increase in the fracture toughness [the crack resistance factor (K_{IC})]; thus for β-SiC films with the grain size of 10–15 nm (the intergrain boundary width of 1–2 nm), K_{IC} is 9.2 ± 2 MPa$^{1/2}$; for ordinary silicon carbide materials, $K_{IC} = 2-6$ MPa$^{1/2}$) (Refs 54 and 58).

The issues of the stability of brittle nanomaterials based on SiC and other refractory compounds are addressed theoretically within the framework of solid-state physics and mechanics (see, *e.g*., Refs 59–61). In particular, such problems as homogeneous and heterogeneous formation of dislocations, origin and propagation of cracks on interfaces, grain boundary sliding, *etc*. were considered.

The *in situ* observation of a plastic deformation in the HRSEM and HRTEM tests of β-SiC nanowires

(70 – 100 nm in diameter) should be considered as the most interesting experimental result.[62, 63] The test temperature was close to room temperature and deformation exceeded 200%; the test revealed an increase in the concentration of dislocations in the initial stage and structural amorphization in the final stage. The results of a computer simulation[64] also deserve mention. A model with the size of $62.5 \times 62.5 \times 53.5$ nm^3 contained 18.7 million atoms, the grain size was 8 nm; this revealed the grain boundary sliding in the first stage of deformation at room temperature followed by the intragrain dislocation shears.

Note that the high-temperature superplasticity of nano-SiC was mentioned as far back as 10 years ago. Figure 10 illustrates the deformation behaviour of β-SiC samples with crystallites measuring ~2 μm and ~0.2 μm at 1800 °C.[65] For coarse-grain samples, this was a typical brittle failure, whereas the objects close to nanostructures exhibited superplasticity (deformation ~110%).

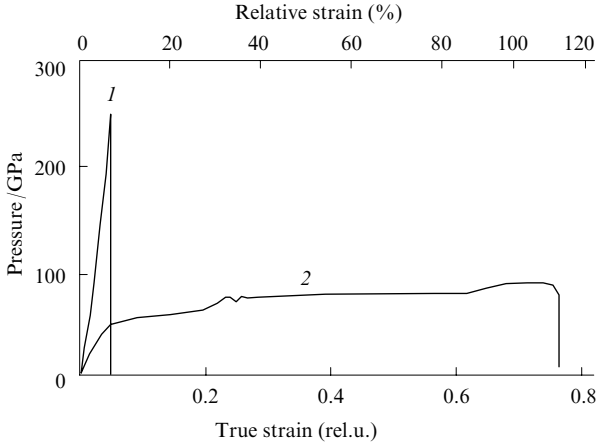


Figure 10. The behaviour of hot-pressed (*1*) and isostatic hot-pressed (*2*) β-SiC samples (with small additions of boron and carbon) in the high-temperature deformation (with the strain rate of 10^{-1} s^{-4}).[65] T = 1800 °C, L /μm: (*1*) 2, (*2*) 0.2.

Note that, as a rule, for common coarse-grain β-SiC samples, the brittle – ductile transition temperature does not drop below 900 – 1200 °C (Ref. 66) (and can be even >1800 °C, according to Fig. 10), *i.e.*, the decrease in this characteristic with the transition to nanostructured materials can be substantial; however, it is difficult to gain such an advantage for bulk nanoobjects, because the technology of their preparation should provide high-quality nanostructures that contain no nano- and micropores nor other defects inside nanograins and especially on their boundaries.

Above, we considered the evolution of PL spectra for 6*H*-SiC with the transition from a coarse-grain substrate to a nanoporous sample and further to isolated nanoparticles (see Fig. 2). Examples of changes in the luminescence and optical properties of nano-SiC (nanoparticles, nanotubes, quantum dots and nanofilms) can be found in a review,[14] which also shows the analysis of results of theoretical studies of this phenomenon. The theory that explains the changes in PL spectra and the broadening of the band gap with the quantum size effect (effect of dimensional quantization) was based on the analysis of the band structure that took into account the finite size of nanocrystals. It is known that the electron excitation energy in nanostructured semiconductors exceeds the energy of interband transition in the corresponding macrocrystalline semiconductors. As applied to nanosilicon, this effect was comprehensively treated in a monograph.[13] According to theoretical estimates, the broadening of the band gap for the 6*H*-SiC hexagonal polytype started with the nanoobject radius below ~7 nm, while its sharp increase started from sizes <3 nm; for the 3*C*-SiC cubic polytype, these values were <4 nm and <1.5 nm, respectively.[14] The cubic polytype was studied most comprehensively (both theoretically and experimentally); thus the band gap for particles with diameters of 3.9 and 8.8 nm were found to be ~2.7 and ~2.3 eV, respectively (the latter value was close to that shown in Table 1).[67]

The *ab initio* calculations of optical properties, chemisorption characteristics and stability of silicon carbide nanotubes of different shapes as a function of their geometrical size and chirality have shown[68 – 71] that NO_2 molecules can be sorbed by silicon carbide nanotubes in contrast, for example, to carbon and boronitride nanotubes, and the nanotube structure stability increases with the increase in the length and the diameter of nanotubes.

An attempt was undertaken[72, 73] to study the electrical and galvanomagnetic properties of amorphous hydrogenized SiC films and epitaxial 3*C*-SiC films. The studies of the effect of annealing of amorphous films on their conductivity revealed the temperature dependence of the activation energy.[72] Figure 11 shows temperature dependences of

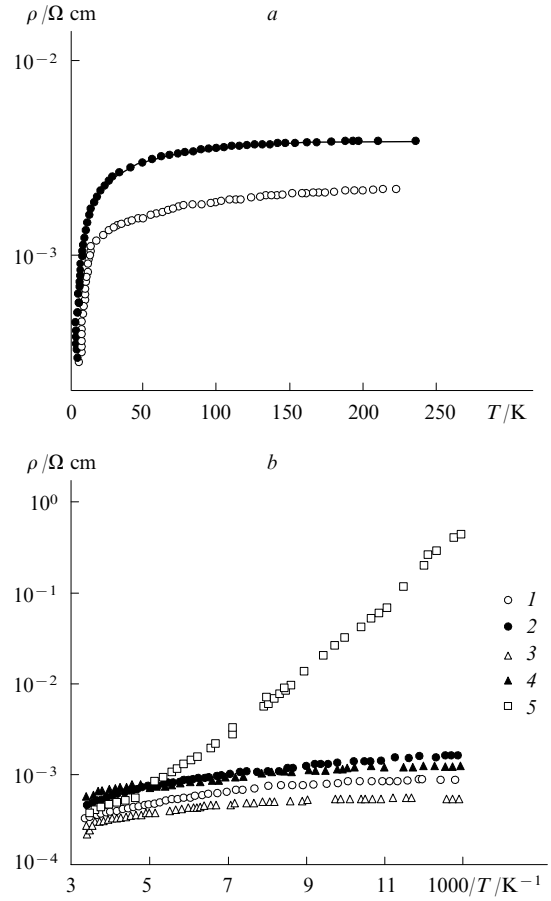


Figure 11. Direct (*a*) and inverse (*b*) temperature dependences of the resistance of 3*C*/6*H* heterostructures.
(*1* – *4*) Heterostructures with different doping levels of the 3*C* layer; (*5*) 6*H* substrate.

specific conductivity for epitaxial films grown on the 6*H*-SiC substrate.[73] It is seen that as the temperature dropped, the electric resistance of the 3*C*-SiC/6*H*-SiC heterostructures increased approximately by the exponential law; for $T < 50$ K, the resistance increased linearly with $T^{1/3}$. At the liquid nitrogen temperature (77 K), the substrate electric resistance (hexagonal polytype) was ~ 2 orders of magnitude higher as compared with films. The studied epitaxial layers exhibited n-type conductivity, the concentration of carriers and their mobility at 300 K were 2×10^{18} cm^{-3} and 40 cm^2 (V s)$^{-1}$, respectively, *i.e.*, sufficiently close to the data in Table 1. Analysis of the results also demonstrated that the low resistance of these layers at liquid helium temperatures may be associated with the presence of the insulator – metal junction.

Information on the electrical and optical properties of the 3*C*-SiC/6*H*-SiC heterostructures and superlattices (multilayer films) on their basis were generalized as regards the problems of electronics in a review.[7]

Recently, studies of the effect of radiation on the properties of nano-SiC have been started. Thus a comparison of structural evolution of 3*C*-SiC samples in their conventional crystalline state (grain size ~ 1 μm, porosity 15%) and with the nanocrystalline structure (grain size ~ 36 nm, porosity 8%) has shown that irradiation with the xenon ions (energy 95 MeV) in a dose of 5×10^{14} cm^{-2} was accompanied by approximately identical variations in the lattice spacing and did not lead to complete structural amorphization.[74] At the same time, it is known that 6*H*-SiC single crystals were actively amorphized under radiation. Changes in the Raman, PL, IR and XRD spectra induced by co-implantation of carbon and aluminium ions into these 6*H*-SiC films were analyzed.[75]

Certain publications (see a review[76] and references therein) contain encouraging results obtained in studying the biological properties of amorphous SiC films as applied to biomedicine. Previous *in vivo* and *in vitro* studies have indicated, forinstance, biocompatibility of SiC with living cells able of capturing and ingesting the foreign particle (phagocytosis). However, the accumulation of systematic information on biological characteristics of nano-SiC is in its very beginning. This is particularly important in the context of the mentioned risk of toxicity of nanoobjects.

IV. Conclusion

Studying the properties of nano-SiC revealed many interesting aspects that, first of all, noteworthy are the possibility of substantial increase in hardness, the manifestation of the high ductility of nanowires, a considerable increase in the intensity of PL spectra, biocompatibility, high resistance against radiation-induced amorphization, *etc*. Conventional application fields of silicon carbide materials (*e.g.*, abrasives and refractory materials, heating elements, superfine powders and fibres, certain semiconductor devices, additives to compositions, *etc*.) have gained impetus to potential extension. Adequate biocompatibility and high wear resistance of nano-SiC made promising the use of these objects as the materials of coatings for implanted microelectrodes, worn joints, highly porous membranes and biosensors.[76] The chemical inertness and biocompatibility together with good optical properties open up the possibilities of using SiC-based quantum dots in the fluorescence diagnostics in medicine.[77] The high potential of nano-SiC-based materials in opto- and nanoelectronics,[7,78] as a part of micro- and nanoelectromechanical systems[79,80] and also as porous high-temperature filters and catalyst carriers is quite evident.[17,19] The high radiation stability of nanostructured silicon carbide materials makes them promising candidates to be used in nuclear technology facilities [*e.g.*, as the blanket and divertor facing material in the International Thermonuclear Experimental Reactor (ITER)[81]].

Realization of the listed applications largely depends on the efficiency of the technology of synthesis of nano-SiC. It is therefore appropriate to mention the development of the method of solid-phase epitaxy of SiC on silicon.[42] It is expected that the thus obtained nano-SiC layers would find application as the substrates, light-emitting diodes and solar cells.[82] The methods of synthesis and consolidation of SiC nanopowders are being developed, for example, the recently proposed interesting carbothermal synthesis (α-SiC polytype), which makes use of spherical SiO_2 particles with a narrow size distribution (2 – 10 nm).[83] Thus, as was noted above, the necessity of comparing different methods of nano-SiC synthesis is still urgent.

At the same time, information on the stability of physicochemical, physicomechanical and, correspondingly, operational characteristics of these materials seems to be insufficient. Moreover, the extension of application fields of nano-SiC certainly requires further development of fundamental studies in the field of size effects.

This review was prepared with the financial support of the Russian Foundation for Basic Research (Projects No. 08-03-00105 and No. 09-03-11000) and also by the Programme of Fundamental Studies of the Presidium of the Russian Academy of Sciences (subprogrammes P-18 and P-27). The author is grateful to V V Klyucharev and S V Klyucharev for their assistance in the preparation of this review for publication and also to D I Tetel'baum for discussion and valuable remarks.

References

1. *Silicon Carbide 2006 — Materials Processing and Devices* Vol. 911 (Eds M Dudley, M Capano, T Kimono, A R Powell, Sh Wang) (Warrendale: Mater. Res. Soc., 2006)
2. *Silicon Carbide and Related Materials. ECSCRM 2006* Vols 556 – 557 (Eds N Wright, C M Johnson, K Vassilevski, I Nikitina, A Horsfall) (Stafa, Zurich: Trans. Tech. Publ., 2007)
3. *Silicon Carbide 2008 — Materials Processing and Devices* Vol. 1069 (Eds M Dudley, C M Johnsohn, A R Powell, S-H Ryu) (Warrendale: Mater. Res. Soc., 2008)
4. R A Andrievski *Usp. Khim.* **74** 1163 (2005) [*Russ. Chem. Rev.* **74** 1061 (2005)]
5. R A Andrievski, in *Handbook of Nanomaterials* (Ed. Y Gogotsi) (Boca Raton, FL: CRC Press, 2006) p. 405
6. R A Andrievski *Ross. Nanotekhn.* **2** (11 – 12) 6 (2007) [a]
7. A A Lebedev *Semicond. Sci. Technol.* **21** R17 (2006)
8. L L Snead, T Nozawa, Y Katoh, T-S Byun, S Kondo, D A Petti *J. Nucl. Mater.* **371** 329 (2007)
9. S A Kukushkin, A V Osipov, V N Bessolov, B K Medvedev, V K Nevolin, K A Tcarik *Rev. Adv. Mater. Sci.* **17** 1 (2008)
10. H Lin, J A Gerbec, M Sushchikh, E W McFarland *Nanotechnology* **19** 325601 (2008)
11. Y Yang, Z-M Lin, J-T Li *J. Eur. Ceram. Soc.* **29** 175 (2009)
12. T Ebadzadeh, E Marzban-Rad *Mater. Character.* **60** 69 (2009)
13. N N Gerasimenko, Yu N Parkhomenko *Kremnii — Material Nanoelektroniki* (Silicon is Material for Nanotechnology) (Moscow: Tekhnosfera, 2007)
14. J Y Fan, X L Wu, P K Chu *Prog. Mater. Sci.* **51** 983 (2006)
15. J Botsoa, J M Bluet, V Lysenko, O Marty, D Barbier, G Guillot *J. Appl. Phys.* **102** 083526 (2007)

16. J Zhu, Z Liu, X L Wu, L L Xu, W C Zhang, P K Chu *Nanotechnology* **18** 365603 (2007)
17. F Kawamura, H Yamane, T Yamada, S Yin, T Sato *J. Am. Ceram. Soc.* **91** 51 (2008)
18. A R Maddocks, D J Cassidy, A S Jones, A T Harris *Mater. Chem. Phys.* **113** 861 (2009)
19. J-S Lee, S-H Lee, S-C Choi *J. Alloys Compd.* **467** 543 (2009)
20. Yu S Nagornov, B M Kostishko, S N Mikov, Sh R Atazhinov, A V Zolotov, E S Pchelintseva *Zh. Tekh. Fiz.* **77** (8) 135 (2007) [b]
21. L-S Liao, X-M Bao, Z-F Yang, N-B Min *Appl. Phys. Lett.* **66** 2382 (1995)
22. Y Z Wan, G Y Xiong, F Song, H L Luo, Y Huang, F He, L B Guo, Y L Wang *Surf. Rev. Lett.* **14** 1103 (2007)
23. D I Tetel'baum, A N Mikhailov, A I Belov, V K Vasil'ev, A I Kovalev, D L Vainshtein, Y Golan, A Osherov *Poverkhnost* (9) 50 (2009) [c]
24. H Liu, G-A Cheng, C Liang, R Zheng *Nanotechnology* **19** 245606 (2008)
25. J Chen, G Yang, R Wu, Y Pan, J Lin, R Zhai, L Wu *J. Nanosci. Nanotechnol.* **8** 2151 (2008)
26. J Wei, K Li, H Li, D Hou, Y Zhang, Ch Wang *J. Alloys Compd.* **462** 271 (2008)
27. F-L Wang, L-Y Zhang, Y-F Zhang *Nanoscale Res. Lett.* **4** 153 (2009)
28. G Attolini, F Rossi, M Bosi, B E Watts, G Salviati *J. Non-Cryst. Solids* **354** 5227 (2008)
29. T Taguchi, N Igawa, H Yamamoto, S Jitsukawa *J. Am. Ceram. Soc.* **88** 459 (2005)
30. Z Xie, D Tao, J Wang *J. Nanosci. Nanotechnol.* **7** 647 (2007)
31. J Deng, K Su, X Wang, Q Zeng, L Cheng, Y Xu, L Zhang *Theor. Chem. Acc.* **122** 1 (2009)
32. D Song, E-C Cho, Y-H Cho, G Conibeer, Y Huang, S Huang, M A Green *Thin Solid Films* **516** 3824 (2008)
33. A V Semenov, V M Puzikov, M V Dobrotvorskaya, A G Fedorov, A V Lopin *Thin Solid Films* **516** 2899 (2008)
34. H X Zhang, P X Feng, V Makarov, B R Weiner, G Morell *Mater. Res. Bull.* **44** 184 (2009)
35. H Colder, R Rizk, M Morales, P Marie, J Vicens *J. Appl. Phys.* **98** 024313 (2005)
36. M Kuenle, S Janz, O Eibl, C Berthold, V Presser, K-G Nickel *Mater. Sci. Eng. B* **159** – **160** 355 (2009)
37. A Tabata, Y Komura, Y Hoshide, T Narita, A Kondo *Jpn. J. Appl. Phys.* **47** 561 (2008)
38. S L Koeng, O Shevaleevskiy *Pure Appl. Chem.* **80** 2141 (2008)
39. X-A Fu, S Noh, L Chen, M Mehregany *J. Nanosci. Nanotechnol.* **8** 5581 (2008)
40. A R Beaber, L J Qi, J Hafiz, P H McMurry, J V R Heberlein, W W Gerberich, S L Girshick *Surf. Coat. Technol.* **202** 871 (2007)
41. V V S S Srikanth, T Staedler, X Jang *Appl. Phys. A: Mater. Sci. Proc.* **91** 149 (2008)
42. S A Kukushkin, A V Osipov *Fiz. Tv. Tela* **50** 1188 (2008) [d]
43. M Imade, T Ogura, M Uemura, F Kawamura, M Yoshimura, Y Kitaoka, T Sasaki, Y Mori, M Yamazaki, Sh Suwabe, Sh-I Nakashima *Mater. Lett.* **63** 649 (2009)
44. R A Andrievski *Materialovedenie* (4) 20 (2006) [e]
45. A A Lebedev, S Yu Davydov *Fiz. Tekh. Poluprovod.* **39** 296 (2005) [f]
46. S Muto, T Tanabe *J. Appl. Phys.* **93** 3765 (2003)
47. V Kulikovsky, V Vorlíček, P Bohač, M Stranyanek, R Čtvrlik, A Kurdyumov, L Jastrabik *Surf. Coat. Technol.* **202** 1738 (2008)
48. E J Oliver, J H Neethling *Int. J. Refr. Met. Hard Mater.* **27** 443 (2009)
49. Y Zhang, H W Shim, H Huang *Appl. Phys. Lett.* **92** 261908 (2008)
50. L N Sorokin, N V Veselov, M P Shcheglov, A E Kalmykov, A A Sitnikov, A A Feoktistov, A V Osipov, S A Kukushkin *Pis'ma Zh. Tekh. Fiz.* **34** (22) 88 (2008) [g]
51. Yu V Trushin, E E Zhurkin, K L Safonov, A A Shmidt, V S Kharlamov, S A Korolev, M N Lubov, J Pezoldt *Pis'ma Zh. Tekh. Fiz.* **30** (15) 48 (2004) [g]
52. K L Safonov, Candidate Thesis in Physical Mathematical Sciences, St Petersburg State Polytechnic University, St Petersburg, 2009
53. F Liao, S L Gershick, W M Mook, W W Gerberich, M R Zachariah *Appl. Phys. Lett.* **86** 171913 (2005)
54. X Zhao, X He, Y Sun, J Yi, P Xiao *Acta Mater.* **57** 893 (2009)
55. N Tymiak, D I Iordanoglu, D Neumann, A Gidwani, F Di Fonzo, M H Fan, N P Rao, W W Gerberich, P H McMurri, J V R Heberlein, S L Girshick, in *Proceedings of the 14th International Symposium on Plasma Chemistry, Prague, 1999* Vol. 3, p. 1989
56. R Vassen, D Stover *Mater. Sci. Eng. A* **301** 59 (2001)
57. R A Andrievski, A M Glezer *Usp. Fiz. Nauk* **179** 337 (2009) [*Physics-Uspekhi* **52** 315 (2009)]
58. X Zhao, R M Langfold, J Tan, P Xiao *Scr. Mater.* **59** 39 (2007)
59. M Yu Gutkin, I A Ovid'ko *Fizicheskaya Mekhanika Deformiruemykh Nanostruktur. Nanokristallicheskie Plenki i Pokrytiya* (Physical Mechanics of Deformated Nanostructure. Films and Covers) (St Petersburg: Yanus, 2005) Vol. 2
60. I A Ovid'ko, A G Sheinerman *Fiz. Tv. Tela* **50** 1002 (2008) [d]
61. N F Morozov, I A Ovid'ko, A G Sheinerman *Dokl. Akad. Nauk* **419** 184 (2008) [h]
62. X D Han, Y F Zhang, K Zheng, X N Zhang, Z Zhang, Y J Hao, X Y Guo, J Yuan, Z L Wang *Nano Lett.* **7** 452 (2007)
63. Y Zhang, X Han, K Zheng, Z Zhang, X Zhang, J Fu, Y Ji, Y Hao, X Guo, Z Wang *Adv. Funct. Mater.* **17** 3435 (2007)
64. I Szlufarska, A Nakano, P Vashishta *Science* **309** 911 (2005)
65. Y Shinodu, T Nagano, H Gu, F Wakai *J. Am. Ceram. Soc.* **82** 2916 (1999)
66. R A Andrievski, I I Spivak *Prochnost' Tugoplavkikh Soedinenii i Materialov na Ikh Osnove* (Strength and Refractoriness of Compounds and Materials Based on Their) (Chelyabinsk: Metallurgiya, 1989)
67. X L Wu, J Y Fan, T Qiu, X Yang, G G Siu, P K Chu *Phys. Rev. Lett.* **94** 026102 (2005)
68. I J Wu, G Y Guo *Phys. Rev. B* **76** 035343 (2007)
69. S-P Huang, D-S Wu, J-M Hu, H Zhang, Z Xie, H Hu, W-D Cheng *Opt. Express* **15** 10947 (2007)
70. G Gao, S H Park, H S Kang *Chem. Phys.* **355** 50 (2009)
71. G Alfieri, T Kimoto *Phys. Status Solidi B* **246** 407 (2009)
72. L Magafas, D Bandekas, A K Boglou, A N Anagnostopoloulos *J. Non-Cryst. Solids* **353** 1065 (2007)
73. A A Lebedev, P L Abramov, N V Agrinskaya, V I Kozub, A N Kuznetsov, S P Lebedev, G A Oganesyan, L M Sorokin, A V Chernyaev, D V Shamshur *Pis'ma Zh. Tekh. Fiz.* **33** (24) 8 (2007) [g]
74. A Audren, I Monnet, Y Leconte, X Portier, L Thome, M Levalois, N Herlin-Boime, C Reynaud *Nucl. Instr. Methods Phys. Res., Sect. B* **266** 2806 (2008)
75. Z C Feng, S C Lien, J H Zhao, X W Sun, W Lu *Thin Solid Films* **516** 5217 (2008)
76. R Yakimova, R M Petoral Jr, G R Yazdi, C Vahlberg, A L Spetz, K Uvdal *J. Phys. D: Appl. Phys.* **40** 6435 (2007)
77. J Botsoa, V Lysenko, A Geloen, O Marty, J M Bluet, G Guillot *Appl. Phys. Lett.* **92** 173902 (2009)
78. N G Wright, A B Horsfall, K Vassilevski *Mater. Today* **11** (1 – 2) 16 (2008)
79. R J Parro, M C Scardelletti, N C Varaljay, S Zimmerman, C A Zorman *Solid-State Electron.* **52** 1647 (2008)
80. V Gimala, J Pezoldt, O Ambacher *J. Phys. D: Appl. Phys.* **40** 6386 (2007)
81. V P Smirnov *Ros. Khim. Zh.* **52** (6) 79 (2008) [i]
82. S A Kukushkin *Ros. Nanotekhnol.* **3** (11 – 12) 46 (2008) [a]
83. A A Zhokhov, V M Masalov, D V Matveev, M Yu Maksimuk, I I Zver'kova, S S Khasanov, S Z Shmurak, A P Kiselev, A V Bazhenov, G A Emel'chenko *Fiz. Tv. Tela* **51** 1626 (2009) [d]

[a] — *Nanotechnol. Russ. (Engl. Transl.)*
[b] — *Tech. Phys. (Engl. Transl.)*
[c] — *J. Surf. Invest. (Engl. Transl.)*
[d] — *Phys. Solid State (Engl. Transl.)*
[e] — *Mater. Sci. (Engl. Transl.)*
[f] — *Semiconductors (Engl. Transl.)*
[g] — *Tech. Phys. Lett. (Engl. Transl.)*
[h] — *Dokl. Phys. (Engl. Transl.)*
[i] — *Mendeleev Chem. J. (Engl. Transl.)*